

Absolute Neutrino Masses*

CARLO GIUNTI

INFN, Sezione di Torino, and Dipartimento di Fisica Teorica, Università di
Torino, Via P. Giuria 1, I-10125 Torino, Italy

The main aspects of the phenomenology of absolute neutrino masses are reviewed, focusing on the limits on neutrino masses obtained in tritium β decay experiments, cosmological observations and neutrinoless double- β decay experiments.

PACS numbers: 14.60.Pq, 14.60.Lm

1. Introduction

Neutrino oscillation experiments have shown that neutrinos are massive and mixed particles, *i.e.* the left-handed components $\nu_{\alpha L}$ of flavor neutrinos ($\alpha = e, \mu, \tau$) are linear combinations of the left-handed components ν_{kL} of neutrinos with masses m_k :

$$\nu_{\alpha L} = \sum_k U_{\alpha k} \nu_{kL}, \quad (1.1)$$

where U is the mixing matrix (see Refs. [1–3]). Neutrino oscillations depend on the elements of the mixing matrix U , which determine the amplitude of the oscillations, and on the squared-mass differences $\Delta m_{kj}^2 \equiv m_k^2 - m_j^2$, which determine the oscillation length.

The results of solar neutrino experiments (Homestake [4], Kamiokande [5], SAGE [6], GALLEX [7], GNO [8], Super-Kamiokande [9] and SNO [10]) and the reactor long-baseline experiment KamLAND [11] imply that there are large $\nu_e \rightarrow \nu_\mu, \nu_\tau$ transitions with a squared-mass difference $\Delta m_{\text{SUN}}^2 \simeq 8 \times 10^{-5} \text{ eV}^2$.

Atmospheric neutrino experiments (Kamiokande [12], IMB [13], Super-Kamiokande [14], Soudan-2 [15] and MACRO [16]) and the accelerator K2K

* Talk presented at the XXIX International Conference of Theoretical Physics “Matter To The Deepest: Recent Developments In Physics Of Fundamental Interactions”, 8-14 September 2005, Ustron, Poland.

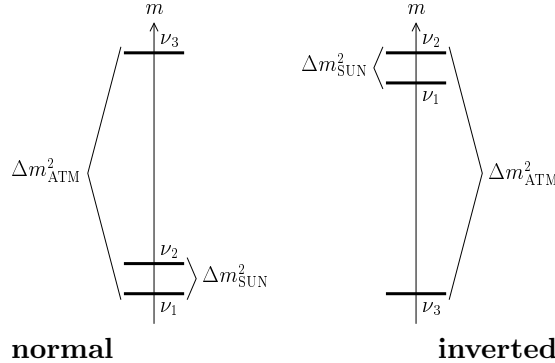


Fig. 1. The two three-neutrino schemes allowed by the hierarchy $\Delta m_{\text{SUN}}^2 \ll \Delta m_{\text{ATM}}^2$.

experiment [17], together with the negative results of the CHOOZ experiment [18], have shown that there are large $\nu_\mu \rightarrow \nu_\tau$ transitions with a squared-mass difference $\Delta m_{\text{ATM}}^2 \simeq 2.5 \times 10^{-3} \text{ eV}^2$.

Since $\Delta m_{\text{ATM}}^2 \gg \Delta m_{\text{SUN}}^2$, at least two independent squared-mass differences are needed in order to explain the results of neutrino oscillation experiments. This requirement is satisfied in the simplest case of three-neutrino mixing, in which the number of massive neutrinos in Eq. (1.1) is three (see Refs. [1–3]). In such a framework, there are two types of possible schemes, which are shown in Fig. 1. We labeled the massive neutrinos in order to have $\Delta m_{21}^2 = \Delta m_{\text{SUN}}^2$ and $|\Delta m_{31}^2| = \Delta m_{\text{ATM}}^2$, with $\Delta m_{32}^2 \simeq \Delta m_{31}^2$. In the normal scheme, which is so-called because it allows a mass hierarchy $m_1 \ll m_2 \ll m_3$, the squared-mass difference Δm_{31}^2 is positive, whereas in the inverted scheme it is negative.

A global fit of the oscillation data [19] gives the best-fits and 3σ ranges for the three-neutrino oscillation parameters listed in Tab. 1. The mixing angles ϑ_{12} , ϑ_{13} , ϑ_{23} belong to the standard parameterization of the mixing matrix [20], in which, with good approximation, ϑ_{12} is the solar mixing angle, ϑ_{23} is the atmospheric mixing angle, and ϑ_{13} is the CHOOZ mixing angle [21, 22]. In Tab. 1 we give only the values of ϑ_{12} and ϑ_{13} , which are sufficient for the following discussion on the phenomenology of absolute neutrino masses.

Neutrino oscillations depend on the differences of neutrino masses, not on their absolute values. As we will see in the following, other experiments are able to give information on the absolute values of neutrino masses. Figure 2 shows the values of the neutrino masses obtained from Δm_{21}^2 and $|\Delta m_{31}^2|$ in Tab. 1 as functions of the unknown value of the lightest mass,

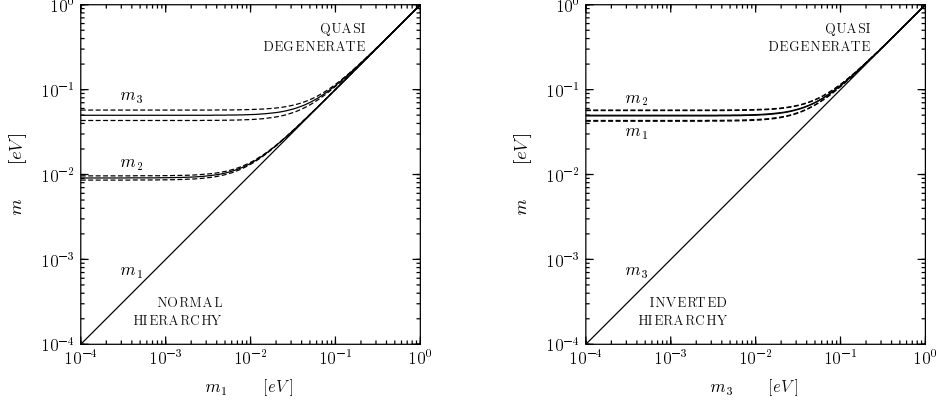


Fig. 2. Values of neutrino masses as functions of the lightest mass m_1 in the normal scheme and m_3 in the inverted scheme. Solid lines correspond to the best-fit in Tab. 1. Dashed lines enclose 3σ ranges.

which is m_1 in the normal scheme and m_3 in the inverted scheme. As shown in the figure, the case $m_3 \ll m_1 \lesssim m_2$ is conventionally called “inverted hierarchy”, whereas in both normal and inverted schemes we have quasi-degeneracy of neutrino masses for $m_1 \simeq m_2 \simeq m_3 \gg \sqrt{\Delta m_{\text{ATM}}^2} \simeq 5 \times 10^{-2}$ eV. In the inverted scheme ν_1 and ν_2 are quasi-degenerate for any value of m_3 and their best-fits values and 3σ ranges are practically superimposed in Figure 2.

In the following, we review the phenomenology of absolute neutrino

Table 1. Best-fit and 3σ range for the three-neutrino oscillation parameters obtained in the global fit of Ref. [19].

Parameter	Best-Fit 3σ Range
Δm_{21}^2	8.3×10^{-5} eV 2 $7.4 \times 10^{-5} - 9.3 \times 10^{-5}$ eV 2
$\sin^2 \vartheta_{12}$	0.28 0.22 – 0.37
$ \Delta m_{31}^2 $	2.4×10^{-3} eV 2 $1.8 \times 10^{-3} - 3.2 \times 10^{-3}$ eV 2
$\sin^2 \vartheta_{13}$	0.01 0 – 0.05

masses in tritium β decay (Section 2), cosmological measurements (Section 3) and neutrinoless double- β decay (Section 4).

2. Tritium β Decay

The measurement of the electron spectrum in β decays provides a robust direct determination of the values of neutrino masses. In practice, the most sensitive experiments use tritium β decay, because it is a super-allowed transition with a low Q -value. Information on neutrino masses is obtained by measuring the Kurie function $K(T)$, given by [23–25]

$$K^2(T) = (Q - T) \sum_k |U_{ek}|^2 \sqrt{(Q - T)^2 - m_k^2}, \quad (2.1)$$

where T is the electron kinetic energy. The effect of neutrino masses can be observed near the end point of the electron spectrum, where $Q - T \sim m_k$. A low Q -value is important, because the relative number of events occurring in an interval of energy ΔT near the end-point is proportional to $(\Delta T/Q)^3$.

In the case of three-neutrino mixing, the Kurie function in Eq. (2.1) depends on three neutrino masses and two mixing parameters (the unitarity of the mixing matrix implies that $\sum_k |U_{ek}|^2 = 1$). However, since so far tritium β decay experiments did not see any effect due to neutrino masses, it is possible to approximate $m_k \ll Q - T$ and obtain

$$K^2(T) \simeq (Q - T) \sqrt{(Q - T)^2 - m_\beta^2}. \quad (2.2)$$

This is a function of only one parameter, the effective neutrino mass m_β , given by [23–29]

$$m_\beta^2 = \sum_k |U_{ek}|^2 m_k^2. \quad (2.3)$$

The current best upper bounds on m_β have been obtained in the Mainz and Troitsk experiments (see Ref. [30]):

$$m_\beta < 2.2 \text{ eV} \quad (95\% \text{ CL}). \quad (2.4)$$

In the near future, the KATRIN experiment [31] will reach a sensitivity of about 0.2 eV.

In the standard parameterization of the mixing matrix we have ($c_{ij} \equiv \cos \vartheta_{ij}$ and $s_{ij} \equiv \sin \vartheta_{ij}$)

$$m_\beta^2 = c_{12}^2 c_{13}^2 m_1^2 + s_{12}^2 c_{13}^2 m_2^2 + s_{13}^2 m_3^2. \quad (2.5)$$

Since the values of Δm_{21}^2 , $|\Delta m_{31}^2|$, ϑ_{12} and ϑ_{13} are determined by neutrino oscillation experiments, there is only one unknown quantity in Eq.(2.5),

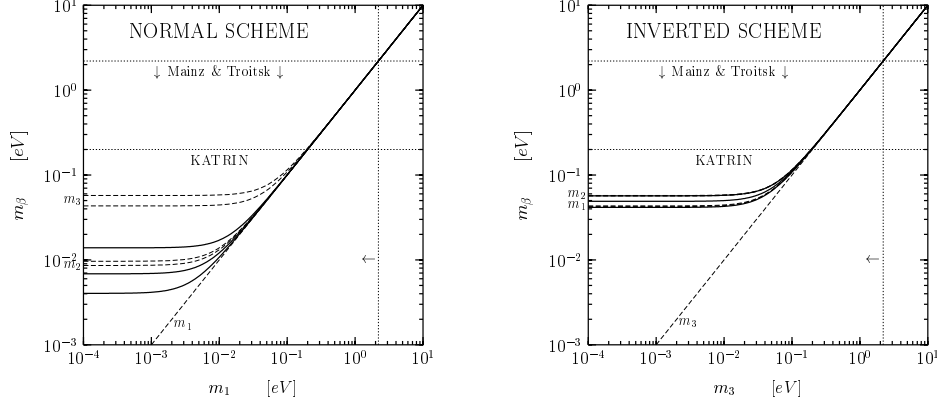


Fig. 3. Effective neutrino mass m_β in tritium β -decay experiments as a function of the lightest mass m_1 in the normal scheme and m_3 in the inverted scheme. Middle solid lines correspond to the best-fit in Tab. 1. Extreme solid lines enclose 3σ ranges. Dashed lines delimit 3σ ranges of individual masses.

which corresponds to the absolute scale of neutrino masses. Figure 3 shows the value of m_β as a function of the unknown value of the lightest mass (m_1 in the normal scheme and m_3 in the inverted scheme), using the values of the oscillation parameters in Tab. 1. The middle solid lines correspond to the best fit and the extreme solid lines delimit the 3σ allowed range. We have also shown with dashed lines the 3σ ranges of the neutrino masses (same as in Fig. 2), which help to understand their contribution to m_β . One can see that, in the case of a normal mass hierarchy (normal scheme with $m_1 \ll m_2 \ll m_3$), the main contribution to m_β is due to m_2 or m_3 or both, because the upper limit for m_β is larger than the upper limit for m_2 . In the case of an inverted mass hierarchy (inverted scheme with $m_3 \ll m_1 \lesssim m_2$), m_β has practically the same value as m_1 and m_2 .

Figure 3 shows that the Mainz and Troitsk experiments and the near-future KATRIN experiment give information on the absolute values of neutrino masses in the quasi-degenerate region in both normal and inverted schemes. In the far future, the inverted scheme could be excluded if experiments with a sensitivity of about 4×10^{-2} eV will not find any effect of neutrino masses.

3. Cosmological Measurements

If neutrinos have masses of the order of 1 eV, they constitute a so-called ‘‘hot dark matter’’, which suppresses the power spectrum of density fluctuations in the early universe at ‘‘small’’ scales, of the order of 1–10

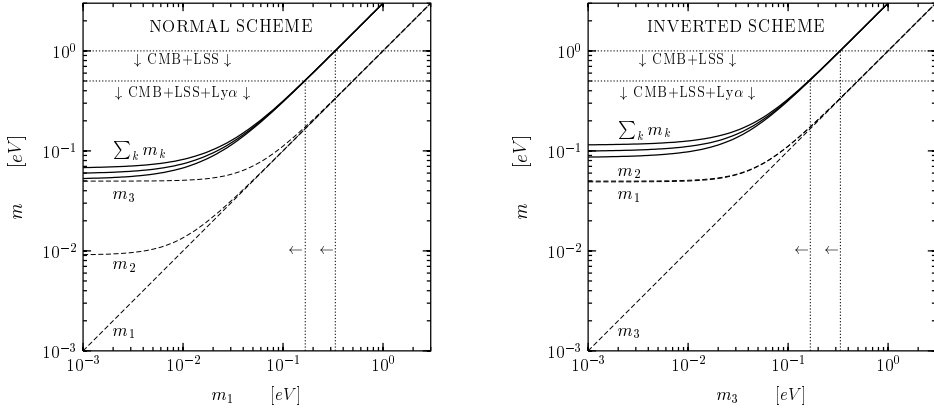


Fig. 4. Sum of neutrino masses as a function of the lightest mass m_1 in the normal scheme and m_3 in the inverted scheme. Middle solid lines correspond to the best-fit in Tab. 1. Extreme solid lines enclose 3σ ranges. Dashed lines show the best-fit values of individual masses.

Mpc (see Ref. [32]). The suppression depends on the sum of neutrino masses $\sum_k m_k$.

Recent high precision measurements of density fluctuations in the Cosmic Microwave Background (WMAP) and in the Large Scale Structure distribution of galaxies (2dFGRS, SDSS), combined with other cosmological data, have allowed to put stringent upper limits on $\sum_k m_k$, of the order of 1 eV [19, 33–38]. However, different authors have obtained significantly different upper bounds, mainly because of the different sets of data considered. The most crucial type of data are the so-called Lyman- α forests, which are constituted by absorption lines in the spectra of high-redshift quasars due to intergalactic hydrogen clouds. Since these clouds have dimensions of the order of 1–10 Mpc, the Lyman- α data are crucial in order to push the upper bound on $\sum_k m_k$ below 1 eV. Unfortunately, the interpretation of Lyman- α data may suffer from large systematic uncertainties. Summarizing the different limits obtained in Refs. [19, 33–38], we estimate the approximate 2σ upper bounds as

$$\sum_k m_k \lesssim 0.5 \text{ eV} \quad (\text{with Ly}\alpha), \quad \sum_k m_k \lesssim 1 \text{ eV} \quad (\text{without Ly}\alpha). \quad (3.1)$$

These limits are shown in Fig. 4, where we have plotted the value of $\sum_k m_k$ as a function of the unknown value of the lightest mass (m_1 in the normal scheme and m_3 in the inverted scheme), using the values of the squared-mass differences in Tab. 1. One can see that both limits in Eq. (3.1) constrain the neutrino masses in the quasi-degenerate region, where the upper bound on

each individual mass is one third of the bound on the sum. In the future, the inverted scheme can be excluded by an upper bound of about 8×10^{-2} eV on the sum of neutrino masses.

4. Neutrinoless Double- β Decay

Neutrinoless double- β decay is a very important process, because it is not only sensitive to the absolute value of neutrino masses, but mainly because it is allowed only if neutrinos are Majorana particles [39, 40]. A positive result in neutrinoless double- β decay would represent a discovery of a new type of particles, Majorana particles. This would be a fundamental improvement in our understanding of nature.

Neutrinoless double- β decays are processes of type $\mathcal{N}(A, Z) \rightarrow \mathcal{N}(A, Z \pm 2) + e^\mp + e^\mp$, in which no neutrino is emitted, with a change of two units of the total lepton number. These processes, which are forbidden in the Standard Model, have half-lives given by (see Refs. [41, 42])

$$T_{1/2}^{0\nu} = (G_{0\nu} |\mathcal{M}_{0\nu}|^2 |m_{\beta\beta}|^2)^{-1}, \quad (4.1)$$

where $G_{0\nu}$ is the phase-space factor, $\mathcal{M}_{0\nu}$ is the nuclear matrix element and

$$m_{\beta\beta} = \sum_k U_{ek}^2 m_k \quad (4.2)$$

is the effective Majorana mass.

A possible indication of neutrinoless double- β decay of ^{76}Ge with half-life

$$T_{1/2}^{0\nu}(^{76}\text{Ge}) = (0.69 - 4.18) \times 10^{25} \text{ y} \quad (3\sigma) \quad (4.3)$$

has been found by the authors of Ref. [43]. Other experiments did not find any indication of neutrinoless double- β decay. The most stringent lower bound on $T_{1/2}^{0\nu}(^{76}\text{Ge})$ has been obtained in the Heidelberg-Moscow experiment [44]:

$$T_{1/2}^{0\nu}(^{76}\text{Ge}) > 1.9 \times 10^{25} \text{ y} \quad (90\% \text{ CL}). \quad (4.4)$$

The IGEX experiment [45] obtained the comparable limit $T_{1/2}^{0\nu}(^{76}\text{Ge}) > 1.57 \times 10^{25} \text{ y}$ (90% CL). Hence, the status of the experimental search for neutrinoless double- β decays is presently uncertain and new experiments which can check the indication (4.3) are needed (see Ref. [42]).

The extraction of the value of $|m_{\beta\beta}|$ from the data has unfortunately a large systematic uncertainty, which is due to the large theoretical uncertainty in the evaluation of the nuclear matrix element $\mathcal{M}_{0\nu}$ (see Refs. [41,

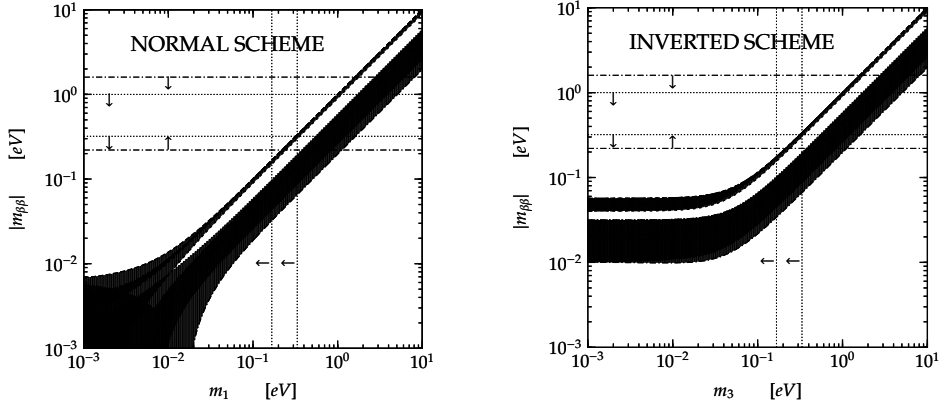


Fig. 5. Effective Majorana mass $|m_{\beta\beta}|$ in neutrinoless double- β decay experiments as a function of the lightest mass m_1 in the normal scheme and m_3 in the inverted scheme. The white areas in the strips need CP violation. The horizontal dotted lines show the interval (4.7) of uncertainty of the current experimental upper bound due to the estimated uncertainty (4.5) of the value of the nuclear matrix element. The horizontal dash-dotted lines delimit the range (4.6) obtained from the indication (4.3). The vertical dotted lines correspond to the cosmological upper bounds on individual neutrino masses in Fig. 4.

42]). In the following, we will use as a 3σ range for the nuclear matrix element $|\mathcal{M}_{0\nu}|$ the interval which covers the results of reliable calculations listed in Tab. 2 of Ref. [42] (other approaches are discussed in Refs. [19, 46–48]):

$$0.41 \lesssim |\mathcal{M}_{0\nu}| \lesssim 1.24, \quad (4.5)$$

which corresponds to a 3σ uncertainty of a factor of 3 for the determination of $|m_{\beta\beta}|$ from $T_{1/2}^{0\nu}(^{76}\text{Ge})$. Using the range (4.5), the indication (4.3) implies

$$0.22 \text{ eV} \lesssim |m_{\beta\beta}| \lesssim 1.6 \text{ eV}, \quad (4.6)$$

and the most stringent upper bound (4.4) implies

$$|m_{\beta\beta}| \lesssim 0.32 - 1.0 \text{ eV}. \quad (4.7)$$

In the standard parameterization of the mixing matrix, the effective Majorana mass is given by

$$m_{\beta\beta} = c_{12}^2 c_{13}^2 m_1 + s_{12}^2 c_{13}^2 e^{i\alpha_{21}} m_2 + s_{13}^2 e^{i\alpha_{31}} m_3, \quad (4.8)$$

where α_{21} and α_{31} are Majorana phases (see Refs. [1–3]), whose values are unknown.

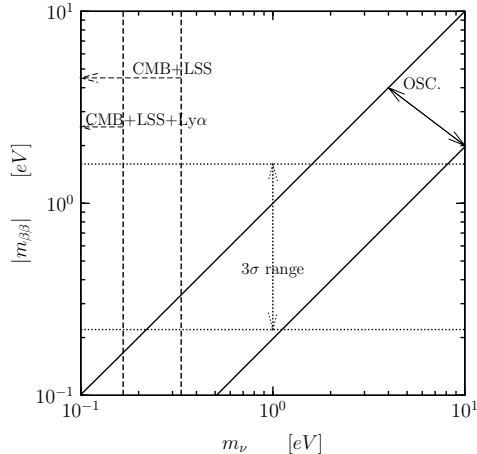


Fig. 6. Allowed regions in the m_ν – $|m_{\beta\beta}|$ plane from the indication of neutrinoless double- β decay with the half-life in Eq. (4.3) (3σ range in Eq. (4.6) between the dotted horizontal lines), oscillation data (allowed range between the diagonal solid lines) and cosmological measurements (upper bounds in Eq. (3.1) represented by the vertical dashed lines). The abscissa $m_\nu \simeq m_1 \simeq m_2 \simeq m_3$ is the scale of quasi-degenerate masses in both normal and inverted schemes.

Figure 5 shows the allowed range for $|m_{\beta\beta}|$ as a function of the unknown value of the lightest mass (m_1 in the normal scheme and m_3 in the inverted scheme), using the values of the oscillation parameters in Tab. 1 (see also Refs. [3,47,49–53]). One can see that, in the region where the lightest mass is very small, the allowed ranges for $|m_{\beta\beta}|$ in the normal and inverted schemes are dramatically different. This is due to the fact that in the normal scheme strong cancellations between the contributions of m_2 and m_3 are possible, whereas in the inverted scheme the contributions of m_1 and m_2 cannot cancel, because maximal mixing in the 1–2 sector is excluded by solar data ($\vartheta_{12} < \pi/4$ at 5.8σ [54]). On the other hand, there is no difference between the normal and inverted schemes in the quasi-degenerate region, which is probed by the present data. From Fig. 5 one can see that, in the future, the normal and inverted schemes may be distinguished by reaching a sensitivity of about 10^{-2} eV.

In Fig. 6 we have enlarged the region of quasi-degenerate masses, which is practically the same in the normal and inverted schemes, in order to assess the compatibility of the indication of neutrinoless double- β decay with the half-life in Eq. (4.3), oscillation data and cosmological measurements. One can see that there is a tension among these sets of data, especially if the cosmological limit with Lyman- α data is considered (see also Ref. [19]).

5. Conclusions

The results of neutrino oscillation experiments have shown that neutrinos are massive particles. However, so far we do not know which is the value of the absolute scale of neutrino masses, except that it is smaller than about 1 eV. Moreover, we do not know if neutrinos are Dirac or Majorana particles. The solution of these fundamental mysteries is one of the hot topics in experimental and theoretical high-energy physics research.

REFERENCES

- [1] S.M. Bilenky, C. Giunti and W. Grimus, *Prog. Part. Nucl. Phys.* **43** (1999) 1, [hep-ph/9812360](#).
- [2] S.M. Bilenky et al., *Phys. Rept.* **379** (2003) 69, [hep-ph/0211462](#).
- [3] C. Giunti and M. Laveder, [hep-ph/0310238](#).
- [4] Homestake, B.T. Cleveland et al., *Astrophys. J.* **496** (1998) 505.
- [5] Kamiokande, Y. Fukuda et al., *Phys. Rev. Lett.* **77** (1996) 1683.
- [6] SAGE, J.N. Abdurashitov et al., *J. Exp. Theor. Phys.* **95** (2002) 181, [astro-ph/0204245](#).
- [7] GALLEX, W. Hampel et al., *Phys. Lett.* **B447** (1999) 127.
- [8] GNO, M. Altmann et al., *Phys. Lett.* **B616** (2005) 174, [hep-ex/0504037](#).
- [9] Super-Kamiokande, J. Hosaka et al., [hep-ex/0508053](#).
- [10] SNO, B. Aharmim et al., [nucl-ex/0502021](#).
- [11] KamLAND, T. Araki et al., *Phys. Rev. Lett.* **94** (2005) 081801, [hep-ex/0406035](#).
- [12] Kamiokande, Y. Fukuda et al., *Phys. Lett.* **B335** (1994) 237.
- [13] IMB, R. Becker-Szendy et al., *Phys. Rev.* **D46** (1992) 3720.
- [14] Super-Kamiokande, Y. Ashie et al., *Phys. Rev.* **D71** (2005) 112005, [hep-ex/0501064](#).
- [15] Soudan-2, W.W.M. Allison et al., *Phys. Rev.* **D72** (2005) 052005, [hep-ex/0507068](#).
- [16] MACRO, M. Ambrosio et al., *Phys. Lett.* **B566** (2003) 35, [hep-ex/0304037](#).
- [17] K2K, E. Aliu et al., *Phys. Rev. Lett.* **94** (2005) 081802, [hep-ex/0411038](#).
- [18] CHOOZ, M. Apollonio et al., *Eur. Phys. J.* **C27** (2003) 331, [hep-ex/0301017](#).
- [19] G.L. Fogli et al., *Phys. Rev.* **D70** (2004) 113003, [hep-ph/0408045](#).
- [20] Particle Data Group, S. Eidelman et al., *Phys. Lett.* **B592** (2004) 1.
- [21] S.M. Bilenky and C. Giunti, *Phys. Lett.* **B444** (1998) 379.
- [22] W.L. Guo and Z.Z. Xing, *Phys. Rev.* **D67** (2003) 053002, [hep-ph/0212142](#).
- [23] R.E. Shrock, *Phys. Lett.* **B96** (1980) 159.
- [24] B.H.J. McKellar, *Phys. Lett.* **B97** (1980) 93.

- [25] I.Y. Kobzarev et al., Sov. J. Nucl. Phys. 32 (1980) 823.
- [26] E. Holzschuh, Rept. Prog. Phys. 55 (1992) 1035.
- [27] C. Weinheimer et al., Phys. Lett. B460 (1999) 219.
- [28] F. Vissani, Nucl. Phys. Proc. Suppl. 100 (2001) 273, [hep-ph/0012018](#).
- [29] Y. Farzan and A.Y. Smirnov, Phys. Lett. B557 (2003) 224, [hep-ph/0211341](#).
- [30] C. Weinheimer, [hep-ex/0210050](#).
- [31] KATRIN, L. Bornschein et al., eConf C030626 (2003) FRAP14, [hep-ex/0309007](#).
- [32] W. Hu, D.J. Eisenstein and M. Tegmark, Phys. Rev. Lett. 80 (1998) 5255, [astro-ph/9712057](#).
- [33] D.N. Spergel et al., Astrophysical Journal Supplement Series 148 (2003) 175, [astro-ph/0302209](#).
- [34] S. Hannestad, JCAP 0305 (2003) 004, [astro-ph/0303076](#).
- [35] O. Elgaroy and O. Lahav, JCAP 04 (2003) 004, [astro-ph/0303089](#).
- [36] SDSS, M. Tegmark et al., Phys. Rev. D69 (2004) 103501, [astro-ph/0310723](#).
- [37] U. Seljak et al., Phys. Rev. D71 (2005) 043511, [astro-ph/0406594](#).
- [38] U. Seljak et al., Phys. Rev. D71 (2005) 103515, [astro-ph/0407372](#).
- [39] J. Schechter and J.W.F. Valle, Phys. Rev. D25 (1982) 2951.
- [40] E. Takasugi, Phys. Lett. B149 (1984) 372.
- [41] O. Civitarese and J. Suhonen, Nucl. Phys. A729 (2003) 867, [nucl-th/0208005](#).
- [42] S.R. Elliott and J. Engel, J. Phys. G30 (2004) R183, [hep-ph/0405078](#).
- [43] H. Klapdor-Kleingrothaus et al., Phys. Lett. B586 (2004) 198, [hep-ph/0404088](#).
- [44] H.V. Klapdor-Kleingrothaus et al., Eur. Phys. J. A12 (2001) 147.
- [45] IGEX, C.E. Aalseth et al., Phys. Rev. D65 (2002) 092007, [hep-ex/0202026](#).
- [46] V.A. Rodin et al., Phys. Rev. C68 (2003) 044302, [nucl-th/0305005](#).
- [47] S. Bilenky, A. Faessler and F. Simkovic, Phys. Rev. D70 (2004) 033003, [hep-ph/0402250](#).
- [48] J.N. Bahcall, H. Murayama and C. Pena-Garay, Phys. Rev. D70 (2004) 033012, [hep-ph/0403167](#).
- [49] F. Feruglio, A. Strumia and F. Vissani, Nucl. Phys. B659 (2003) 359, [hep-ph/0201291](#).
- [50] F.R. Joaquim, Phys. Rev. D68 (2003) 033019, [hep-ph/0304276](#).
- [51] S. Pascoli and S.T. Petcov, Phys. Lett. B580 (2004) 280, [hep-ph/0310003](#).
- [52] J.N. Bahcall, H. Murayama and C. Pena-Garay, Phys. Rev. D70 (2004) 033012, [hep-ph/0403167](#).
- [53] S.T. Petcov, New J. Phys. 6 (2004) 109.
- [54] J.N. Bahcall, M.C. Gonzalez-Garcia and C. Pena-Garay, JHEP 08 (2004) 016, [hep-ph/0406294](#).